Texture contribution to the anisotropy of physical properties



1994 J. Phys.: Condens. Matter 6 8503

(http://iopscience.iop.org/0953-8984/6/41/012)

J. Phys.: Condens. Matter 6 (1994) 8503–8512. Printed in the UK

# Texture contribution to the anisotropy of physical properties

S V Divinski and V N Dnieprenko
Institute of Metal Physics, Ukrainian Academy of Sciences, Vernadskogo 36, Kiev-142, 252680, Ukraine

Received 28 October 1993, in final form 20 April 1994

**Abstract.** A method has been developed to calculate the texture contribution to the anisotropy of the physical properties of polycrystalline materials. It starts from an approach proposed earlier for modelling the rolling textures in FCC and BCC metals by a superposition of partial fibre components. The averaged values of the elastic constants and Young's modulus have been calculated for copper sheets with different textures. The method computes the component-by-component physical property anisotropy and thus predicts the required component ratios for any required anisotropy. In our approach the texture is described by the minimum number of components, with the number of lasts being rigorously equal to the number of structure components.

## 1. Introduction

The anisotropy of physical properties is a well known feature of most metallic single crystals. In polycrystals, the value of a physical property in an arbitrary direction will also be determined by the grain distribution or texture.

A number of methods exist for calculating the texture contribution to the physical property anisotropy. Some of them [1, 2] use an analytical presentation of the texture spread. Unfortunately, such methods have currently been developed for axial textures only. In the Bunge [3] method the texture contribution to the physical property anisotropy is computed by the coefficients $C_l^{mn}$ of a series expansion of the orientation distribution function (ODF). The ODF is usually reproduced from pole figure data [4]. However, simulation of real ODFs is required for analysing the texture quantitatively. Moreover, the problem of the determination of the optimum texture for any required anisotropy can be solved by a proper choice of the number of components and their dispersions. In practice, the quantitative texture parameters can be changed by variation in the deformation conditions (temperature, deformation rate, etc) [5].

Thus, the faithful simulation of the texture by a proper number of components is needed for prediction purposes. From our point of view, the choice of texture components must be based on both texture and microstructure data. Microstructure elements with close substructure types turn out to have close orientations [6, 7]. In this case each structure type may be attributed to a specific texture component. This correlation of orientation and structure can be established only if any texture component is considered as a limited fibre component (LFC) with an anisotropic spread with respect to the maximum [8, 9]. The LFC concept was qualitatively proposed by Wassermann and Grewen [5] many years ago. This concept starts from the well known presentations of axial textures, which exhibit full axial symmetry. However, unlike the lasts the LFC dispersion may be given by a set of grain rotations with respect to some axis in a limited angular range less than $2\pi$. This approach

0953-8984/94/418503+10$19.50  

turns out to be very useful for the quantitative approximation of most experimental textures [8, 9]. In our opinion, in the case of texture approximation by spherical distributions in [10–12], such demarcation of structure elements over the texture components may be realized with difficulty and is less justified from a physical point of view. Also, in the approach in [8, 9] the texture is described by a much smaller number of parameters as in [10–12].

A method is derived in the present paper for component-by-component averaging of the properties of textured materials using the minimum number of components, which correspond rigorously to the texture and structure types observed experimentally. Copper sheets rolled at different temperatures and, thus, with different textures are studied as an example.

## 2. Theory

Consideration of the dispersion of each texture component with respect to its own 'local' coordinate system, which is rigidly connected with this component, is the main feature of our approach. It is convenient to choose the so-called texture axes of the LFCs [5] as the Oz axes of these 'local' coordinate systems [9]. The texture axis positions correlate with regions of abnormally high values of the pole density in some experimental pole figures [8, 9]. The abnormally high maxima manifest themselves on the pole figures, the indices of which coincide with those of the crystallographic directions of the texture axes. To indicate the position of the component texture axis in an explicit form and to emphasize the importance of such presentations for the description of component spread the designation $(hkl)[uvw]|u'v'w'|$ is introduced for the component, the $(hkl)$ direction of which coincides with the rolling plane, and the $[uvw]$ direction with the rolling direction (RD); $|u'v'w'|$ is the crystallographic direction of the texture axis. In our approach the ODF of a component must be calculated in its 'local' coordinate system, and the following analytical form has been found to correspond well to the experimental data [9]:

$$f(\gamma_1, \gamma_2, \gamma_3) = A \exp\left(-\frac{\gamma_2^2}{2\sigma_1^2}\right) \exp\left[-\frac{1}{2}\left(\frac{|\gamma_1 + \gamma_3| - \sigma_3 + |\sigma_3 - |\gamma_1 + \gamma_3||}{2\sigma_2}\right)^2\right]$$
$$= f_1(\gamma_2) f_2(\gamma_1 + \gamma_3) \tag{1}$$

where $f_1(\gamma_2)$ and $f_2(\gamma_1 + \gamma_3)$ are the corresponding exponents with the normalization coefficients. A set of Eulerian angles $g_\gamma = (\gamma_1, \gamma_2, \gamma_3)$ specifies the grain orientation in the 'local' coordinate system (with respect to the component texture axis); $\sigma_1$, $\sigma_2$ and $\sigma_3$ are the spread parameters. The $\sigma_3$-value determines the length of a region in orientation space with a constant orientation density. By such means one can simulate the so-called orientation tubes, which may be considered as LFC parts [8, 9]. Hereafter any set of three Eulerian angles is determined as specified by Bunge [4]: the coordinate system is first rotated around the Oz axis, then around the new direction of the Ox axis, and finally once again around the Oz axis in its final position.

Then, the total ODF $f_B(g_B)$, which is defined in the space of the standard Eulerian angles $g_B(\varphi_1, \Phi, \varphi_2)$ (in the Bunge notations) with respect to the external coordinate system of the sample, can be calculated as the sum

$$f_B(\varphi_1, \Phi, \varphi_2) = \sum_{k=1}^{N} \frac{p_k}{M_k} \sum_{l=1}^{M_k} f(\gamma_1^{(kl)}, \gamma_2^{(kl)}, \gamma_3^{(kl)}) \tag{2}$$

where the values of the angles $\gamma_1^{(kl)}$, $\gamma_2^{(kl)}$ and $\gamma_3^{(kl)}$ can be determined from

$$g_\gamma^{(kl)} = (g_0^{(kl)})^{-1} g_B (g_1^{(kl)})^{-1}. \tag{3}$$

Here $p_k$ is the volume fraction of the $k$th texture component, $\sum_{k=1}^{N} p_k = 1$; $l$ is the index numbering subsequently equivalent orientations of the $k$th component; $M_k$ is the number of such orientations; the matrix of rotations $g_0^{(kl)}$ defines a transition to the 'local' coordinate system of the texture axis of the $l$th equivalent orientation in the $k$th texture component, and $g_1^{(kl)}$ specifies the orientation of this component in the sample's coordinate system; finally $g_\gamma^{(kl)}$ is the matrix of rotations by the Eulerian angles $\gamma_1^{(kl)}$, $\gamma_2^{(kl)}$, $\gamma_3^{(kl)}$.

The correspondence of model and experimental textures may be considered as a method of texture parameter determination. Now, the texture contribution to the elastic modulus anisotropy in polycrystals may be theoretically determined by averaging single-crystal characteristics over the grain orientations in the sample.

Let $S_{ijkl}^0$ be the tensor of compliances in the coordinate system of the elementary cell of grain. Then, in the sample coordinate system we have

$$S_{mnpq} = \alpha_{mi}\alpha_{nj}\alpha_{pk}\alpha_{ql} S_{ijkl}^0 \tag{4}$$

where $\alpha_{mi}$ are the directional cosines. For the cubic symmetry after simplifications we have

$$\begin{aligned}
&S_{iiii} = S_{1111}^0 - 2s^0(\alpha_{i1}^2\alpha_{i2}^2 + \alpha_{i1}^2\alpha_{i3}^2 + \alpha_{i2}^2\alpha_{i3}^2) && i = 1,2,3 \\
&S_{iijj} = S_{1122}^0 + s^0(\alpha_{i1}^2\alpha_{j1}^2 + \alpha_{i2}^2\alpha_{j2}^2 + \alpha_{i3}^2\alpha_{j3}^2) && i,j = 1,2,3 \qquad i \neq j \\
&S_{ijij} = S_{2323}^0 + s^0(\alpha_{i1}^2\alpha_{j1}^2 + \alpha_{i2}^2\alpha_{j2}^2 + \alpha_{i3}^2\alpha_{j3}^2) && i,j = 1,2,3 \qquad i \neq j \\
&S_{ijkl} = s^0(\alpha_{i1}\alpha_{j1}\alpha_{k1}\alpha_{l1} + \alpha_{i2}\alpha_{j2}\alpha_{k2}\alpha_{l2} + \alpha_{i3}\alpha_{j3}\alpha_{k3}\alpha_{l3}) \\
&\qquad i,j,k,l = 1,2,3 \qquad i \neq j, k \neq 1 \\
&s^0 = S_{1111}^0 - S_{1122}^0 - 2S_{2323}^0.
\end{aligned} \tag{5}$$

Since the grains are distributed on orientations in accordance with $f_B(g_B)$, the averaged tensor $\langle S_{mnpq} \rangle$ of the compliances will be

$$\langle S_{mnpq} \rangle = \frac{1}{8\pi^2} \int f_B(g_B) S_{mnpq} \, dg_B. \tag{6}$$

Thus, the problem is reduced to the calculation of the three-dimensional integral, equation (6), which is quite troublesome. However, if we take into account that, in our approach, the ODF $f_B(g_B)$ is virtually a function of two independent variables, namely $\gamma_2$ and $\gamma_1 + \gamma_3$ (see (1)), then the three-dimensional integral can be reduced to a product of two one-dimensional integrals.

For given values of dispersion of the $k$th texture component the $g_B$ matrix of rotation or, equivalently, the directional cosines $\alpha_{mi}$ from (4) and (5) will be determined by

$$g_B = g_0^{(kl)} g_\gamma g_1^{(kl)} \tag{7}$$

which follows directly from (3). Since elements of the matrices $g_0^{(kl)}$ and $g_1^{(kl)}$ are constants, which are defined by the crystallographic orientation of the $k$th texture component and its texture axis, the directional cosines $\alpha_{mi}$ may be written in the following form:

$$\alpha_{mi} = \sum_s T_s^{(1)}(\gamma_1) T_s^{(2)}(\gamma_2) T_s^{(3)}(\gamma_3). \tag{8}$$

$T_s^{(i)}(\gamma_i)$ are trigonometric functions (sines or cosines) for $\gamma_i$, $i = 1, 2, 3$.

One remark must be made. A set of equivalent orientations indicated in (2) and (3) by the index $l$ exists for each texture component. While these orientations correspond to different maxima in the Eulerian space, they are physically indistinguishable. Thus, it is enough to sum only over the texture components $k$ in equation (6).

In averaging (5) by the type (6) the problem is reduced to averaging different directional cosine combinations upon the texture. Substituting $\alpha_{mi}$ in (6) by its values from (5) we may obtain the following expressions:

$$\langle \ldots \rangle = \sum_k \frac{p_k}{8\pi^2} \sum_s a_s \int_0^\pi f_1(\gamma_2) \sin^{m_s} \gamma_2 \cos^{n_s} \gamma_2 \sin \gamma_2 \, d\gamma_2 \times \int_{-\pi}^{\pi} \int_{-\pi}^{\pi} f_2(\gamma_1 + \gamma_3) \sin^{p_s} \gamma_1 \cos^{q_s} \gamma_1 \sin^{t_s} \gamma_3 \cos^{r_s} \gamma_3 \, d\gamma_1 \, d\gamma_3. \tag{9}$$

Here the symbol $\langle \ldots \rangle$ denotes any combination of the directional cosines of the $\langle \alpha_{mi}\alpha_{nj}\alpha_{pk}\alpha_{ql} \rangle$ type from (5), which is averaged upon the texture. The powers satisfy the following conditions: $m_s + n_s \leqslant 4$, $p_s + q_s \leqslant 4$ and $t_s + r_s \leqslant 4$. Taking into account the explicit form of $f_2(\gamma_1 + \gamma_3)$ the two-dimensional integral (9) can be reduced to a one-dimensional integral by the variable change $u = \gamma_1 + \gamma_3$, $v = \gamma_1 - \gamma_3$ and by subsequent analytical integration with respect to $v$. Then we have

$$\langle \ldots \rangle = \sum_k \frac{p_k}{8\pi^2} \sum_s \int_0^\pi f_1(\gamma_2) \sin^{m_s+1} \gamma_2 \cos^{n_s} \gamma_2 \, d\gamma_2 \int_{-2\pi}^{2\pi} f_2(u)(a_s u + b_s) \sin^{p_s} u \cos^{q_s} u \, du. \tag{10}$$

Here the relation $p_s + q_s \leqslant 8$ holds for the powers $p_s$ and $q_s$. Because of the huge number of the items in (10) all the analytical transformations have been carried out by computer.

The one-dimensional integrals over $\gamma_2$ and $u$ in (10) can be computed for the given dispersion parameters of texture components. The number of the integrals, which have to be calculated numerically, decreases when trigonometric identities are used and for the case under consideration, i.e. metals with a cubic lattice, it is nine over $\gamma_2$ and 19 over $u$.

The tensor of the elastic moduli for rolling textures of cubic metals is known to have orthotropic symmetry which can be characterized by nine non-zero constants. However, the symmetry may be lower for separate components. Thus, we must use a general expression for Young's modulus $\langle E \rangle$ of textured material (the direction is specified by the directional

**Table 1.** Component composition of rolling textures of copper at different temperatures.

| Rolling temperature (K) | Partial fibre component | | | Volume part | grad | | |
|---|---|---|---|---|---|---|---|
| | $\{hkl\}$ | $\langle uvw \rangle$ | $\lvert u'v'w' \rvert$ | $p_k$ | $\sigma_1$ | $\sigma_2$ | $\sigma_3$ |
| 300 | {110} | $\langle 1\bar{1}2 \rangle$ | $\lvert 1\bar{1}1 \rvert$ | 0.505 | 5.2 | 5 | 20 |
| | {112} | $\langle 11\bar{1} \rangle$ | $\lvert 111 \rvert$ | 0.395 | 4.6 | 5 | 12 |
| | {110} | [001] | $\lvert 110 \rvert$ | 0.075 | 6 | 20 | 10 |
| | {001} | [100] | {001} | 0.025 | 7 | 8 | 0 |
| 77 | {110} | $\langle 1\bar{1}2 \rangle$ | $\lvert 1\bar{1}1 \rvert$ | 0.674 | 7.5 | 14 | 0 |
| | {112} | $\langle 11\bar{1} \rangle$ | $\lvert 111 \rvert$ | 0.131 | 6 | 10 | 15 |
| | {110} | [001] | $\lvert 110 \rvert$ | 0.195 | 8 | 10 | 25 |

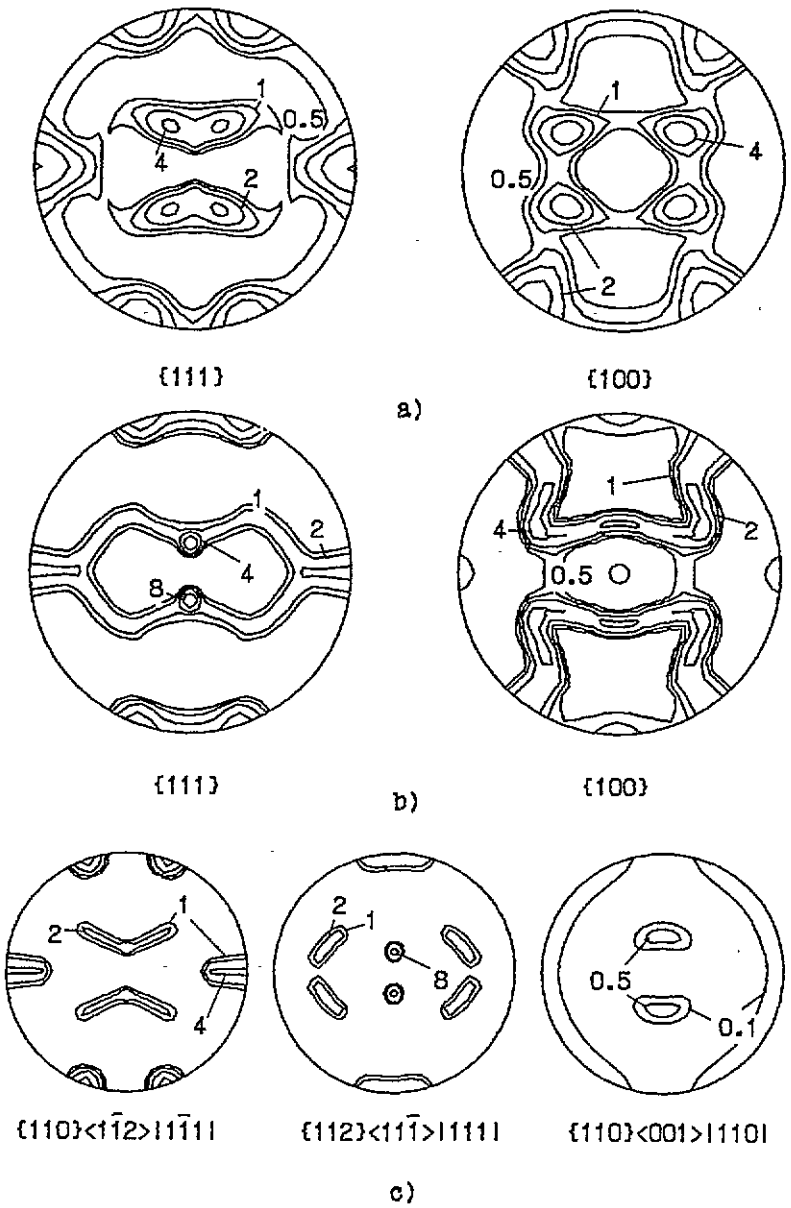


**Figure 1.** The model pole figures {111} and {100} for copper rolled at (a) 77 K and (b) 300 K. (c) The decomposition of the model pole figure {111} for copper rolled at 300 K into separate components.

cosines $\beta_1$, $\beta_2$ and $\beta_3$):

$$\frac{1}{\langle E\rangle} = S^0_{1111} - S^0\Bigg(\sum_{k\neq l}\beta_k^2\beta_l^2(1-3\Delta_{kkll}) + \sum_k \Delta_{kkkk}\beta_k^4 - 2\sum_k\sum_{m\neq l}\Delta_{kkml}\beta_k^2\beta_m\beta_l$$

$$- \Delta_{2313}\beta_1\beta_2\beta_3^2 - \Delta_{2312}\beta_1\beta_2^2\beta_3 - \Delta_{1312}\beta_1^2\beta_2\beta_3\Bigg) \qquad (11)$$

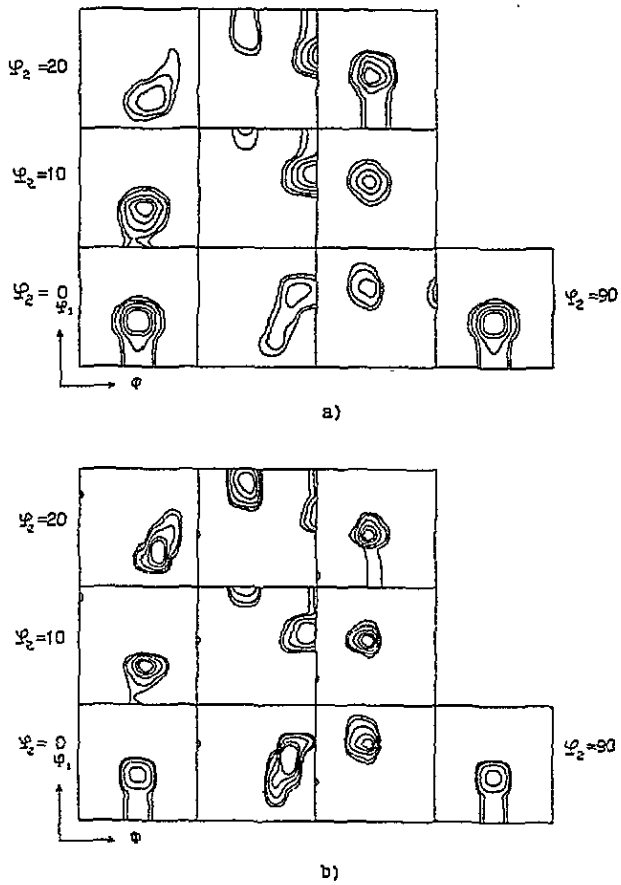


**Figure 2.** The sections of model ODFs by $\varphi_2$ = constant planes for copper rolled at (a) 77 K and (b) 300 K. The intensity levels are 1, 2, 5, 10 and 15.

where $\Delta_{klmn} = \langle \sum_{i=1}^{3} \alpha_{ki}\alpha_{li}\alpha_{mi}\alpha_{ni} \rangle$, $k, l, m, n = 1, 2, 3$.

The Reuss approximation is used in the present work to determine the averaged macroscopic characteristics of the polycrystal sample. In employing the Voigt approximation the compliance tensor $S_{ijkl}$ must be replaced by the elastic modulus tensor $C_{ijkl}$ in equations (5)–(10). The directional cosines $\alpha_{mi}$ are averaged identically. Moreover, to calculate Young's modulus, one additional expression is needed to transform $\langle C_{ijkl} \rangle$ into $\langle S_{ijkl} \rangle$.

## 3. Results and discussion

Anisotropy of the compliances and Young's modulus of the main texture components of copper sheets rolled at 300 and 77 K has been examined. The spread parameters, from which the experimental pole figures were approximated, are listed in table 1. The volume fractions and crystallographic orientations of separate texture components are also presented in table 1.

In this case the distribution of pole densities $P_{\{\bar{H}\}}(\bar{y})$ for a pole figure $\{\bar{H}\}$ and for the ODF (1) can be calculated from

$$P_{\{\bar{H}\}}(\bar{y}) = \sum_{i=1}^{M} \sum_{k=1}^{N} \frac{p_k}{2\pi M} \int_0^{2\pi} f(\gamma_1^{(ik)}, \gamma_2^{(ik)}, \gamma_3^{(ik)}) \, \mathrm{d}\delta \tag{12}$$

**Table 2.** Averaged compliances $\langle S_{pq} \rangle$ for separate texture components and the total textures for copper plates rolled at different temperatures. SCD indicates the single-crystal data.

| Temp. (K) | Rolling temp. (K) | Partial fibre component | $\langle S_{11} \rangle$ | $\langle S_{22} \rangle$ | $\langle S_{33} \rangle$ | $\langle S_{12} \rangle$ | $\langle S_{13} \rangle$ | $\langle S_{23} \rangle$ | $\langle S_{44} \rangle$ | $\langle S_{55} \rangle$ | $\langle S_{66} \rangle$ |
|---|---|---|---|---|---|---|---|---|---|---|---|
| 79 | SCD | | 1.378 | | | −0.571 | | | 1.236 | | |
| | 77 | $\{110\}\langle 1\bar{1}2\rangle\|1\bar{1}1\|$ | 0.837 | 0.620 | 0.726 | −0.247 | −0.354 | −0.136 | 2.975 | 2.104 | 2.530 |
| | | $\{112\}\langle 11\bar{1}\rangle\|111\|$ | 0.727 | 0.571 | 0.729 | −0.166 | −0.324 | −0.168 | 2.847 | 2.222 | 2.854 |
| | | $\{110\}\langle 001\rangle\|110\|$ | 0.597 | 0.724 | 0.717 | −0.184 | −0.177 | −0.304 | 2.305 | 2.811 | 2.785 |
| | | Total | 1.086 | 0.637 | 0.728 | −0.380 | −0.470 | −0.212 | 3.435 | 1.639 | 2.002 |
| | 300 | $\{110\}\langle 1\bar{1}2\rangle\|1\bar{1}1\|$ | 0.695 | 0.639 | 0.719 | −0.190 | −0.269 | −0.213 | 2.667 | 2.443 | 2.760 |
| | | $\{112\}\langle 11\bar{1}\rangle\|111\|$ | 0.705 | 0.592 | 0.719 | −0.171 | −0.298 | −0.185 | 2.779 | 2.327 | 2.836 |
| | | $\{110\}\langle 001\rangle\|110\|$ | 0.547 | 0.719 | 0.716 | −0.157 | −0.154 | −0.326 | 2.217 | 2.903 | 2.891 |
| | | Total | 1.112 | 0.636 | 0.721 | −0.395 | −0.481 | −0.471 | 3.501 | 1.597 | 1.938 |
| 300 | SCD | | 1.500 | | | −0.628 | | | 1.320 | | |
| | 77 | $\{110\}\langle 1\bar{1}2\rangle\|1\bar{1}1\|$ | 0.904 | 0.664 | 0.781 | −0.271 | −0.389 | −0.485 | 3.238 | 2.277 | 2.748 |
| | | $\{112\}\langle 11\bar{1}\rangle\|111\|$ | 0.782 | 0.610 | 0.784 | −0.182 | −0.356 | −0.184 | 3.096 | 2.407 | 3.105 |
| | | $\{110\}\langle 001\rangle\|110\|$ | 0.639 | 0.778 | 0.771 | −0.201 | −0.194 | −0.333 | 2.499 | 3.057 | 3.028 |
| | | Total | 1.178 | 0.682 | 0.783 | −0.417 | −0.517 | −0.216 | 3.745 | 1.764 | 2.165 |
| | 300 | $\{110\}\langle 1\bar{1}2\rangle\|1\bar{1}1\|$ | 0.747 | 0.685 | 0.773 | −0.208 | −0.295 | −0.233 | 2.898 | 2.651 | 3.001 |
| | | $\{112\}\langle 11\bar{1}\rangle\|111\|$ | 0.758 | 0.633 | 0.774 | −0.187 | −0.327 | −0.202 | 3.022 | 2.524 | 3.084 |
| | | $\{110\}\langle 001\rangle\|110\|$ | 0.584 | 0.773 | 0.770 | −0.716 | −0.168 | −0.357 | 2.402 | 3.159 | 3.146 |
| | | Total | 1.207 | 0.682 | 0.776 | −0.434 | −0.528 | −0.343 | 3.818 | 1.719 | 2.095 |
| 500 | SCD | | 1.660 | | | −0.705 | | | 1.475 | | |
| | 77 | $\{110\}\langle 1\bar{1}2\rangle\|1\bar{1}1\|$ | 0.999 | 0.733 | 0.863 | −0.309 | −0.440 | −0.173 | 3.601 | 2.536 | 3.058 |
| | | $\{112\}\langle 11\bar{1}\rangle\|111\|$ | 0.864 | 0.673 | 0.866 | −0.210 | −0.404 | −0.212 | 3.445 | 2.680 | 3.454 |
| | | $\{110\}\langle 001\rangle\|110\|$ | 0.705 | 0.860 | 0.852 | −0.232 | −0.224 | −0.378 | 2.782 | 3.401 | 3.369 |
| | | Total | 1.303 | 0.754 | 0.865 | −0.471 | −0.582 | −0.327 | 4.164 | 1.967 | 2.411 |
| | 300 | $\{110\}\langle 1\bar{1}2\rangle\|1\bar{1}1\|$ | 0.825 | 0.757 | 0.854 | −0.239 | −0.336 | −0.268 | 3.224 | 2.950 | 3.339 |
| | | $\{112\}\langle 11\bar{1}\rangle\|111\|$ | 0.837 | 0.699 | 0.855 | −0.216 | −0.371 | −0.233 | 3.362 | 2.810 | 3.431 |
| | | $\{110\}\langle 001\rangle\|110\|$ | 0.644 | 0.854 | 0.850 | −0.199 | −0.195 | −0.405 | 2.675 | 3.514 | 3.499 |
| | | Total | 1.335 | 0.753 | 0.857 | −0.490 | −0.594 | −0.127 | 4.245 | 1.917 | 2.334 |

where $g_\gamma^{(ik)} = (g_0^{(k)})^{-1} g_B^{(i)} \Omega(\delta) (g_1^{(k)})^{-1}$; $g_B^{(i)}$ is the matrix of rotations of grains to orientations for which $\bar{y} = \bar{h}_i g_B^{(i)}$, where $\bar{h}_i$, $i = 1, \ldots, M$, are the equivalent planes from the $\{\bar{H}\}$ family; $\Omega(\delta)$ is the matrix of rotations by the angle $\delta$ around the $\bar{y}$ direction. The rest of the symbols are the same as in (2) and (3). Model pole figures {111} for different rolling temperatures are shown in figures 1(a) and 1(b). It is seen that they are in good agreement with the pole figures observed experimentally (see, e.g, [5, 13]). In figure 1(c) the decomposition of the {111} model pole figure for copper rolled at 300 K into the separate LFCs is presented. Hereafter the sum of two symmetric components $(110)[1\bar{1}2]|1\bar{1}1|$ and $(110)[\bar{1}\bar{1}2]|\bar{1}\bar{1}1|$ (or $(112)[11\bar{1}]|111|$ and $(112)[\bar{1}\bar{1}1]|111|$) is considered as a unified component $\{1\bar{1}0\}\langle 1\bar{1}2\rangle|1\bar{1}1|$ (or $\{112\}\langle 11\bar{1}\rangle|111|$, respectively). This is convenient for studying the physical property anisotropy of the separate components, since these symmetric components have a common nature of formation and development. Moreover, each symmetric component mentioned above taken separately has a symmetry lower than the orthotropic symmetry. In this case, it was established that the nine non-zero elastic constants, which characterize the orthotropic symmetry, coincide for symmetric components, but other non-zero constants have the same magnitudes and opposite signs and vanish under summation. In figure 1(c) the pole figures for the separate components are presented with allowance for their volume fractions in the total texture (figure 1(b)).

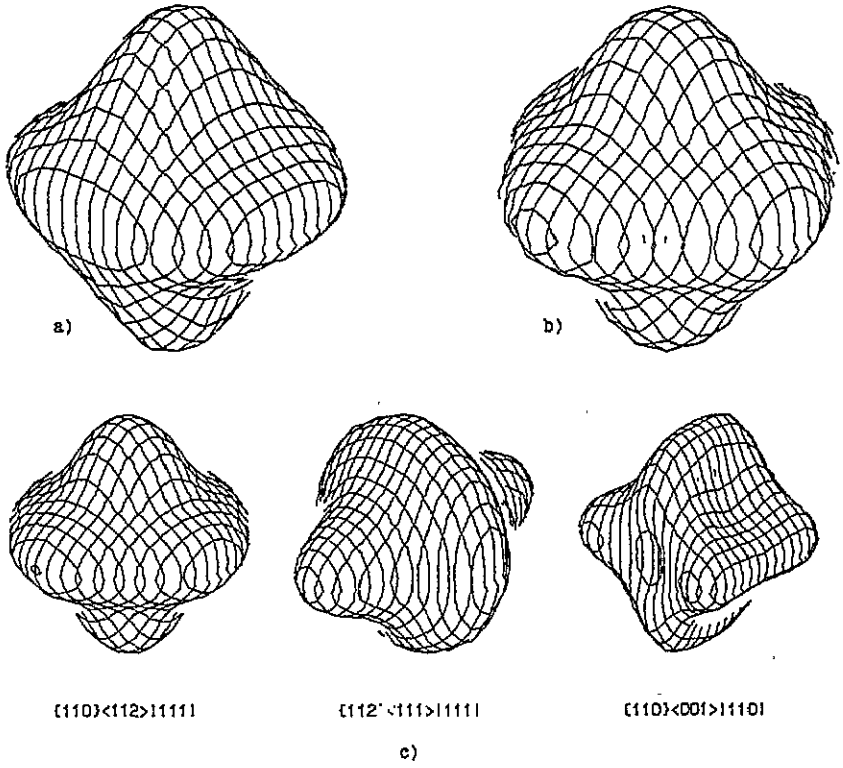


**Figure 3.** Three-dimensional images of the anisotropy of Young's modulus for copper plates rolled at (a) 77 K and (b) 300 K and (c) the same for the separate components of the texture of rolling at 300 K.

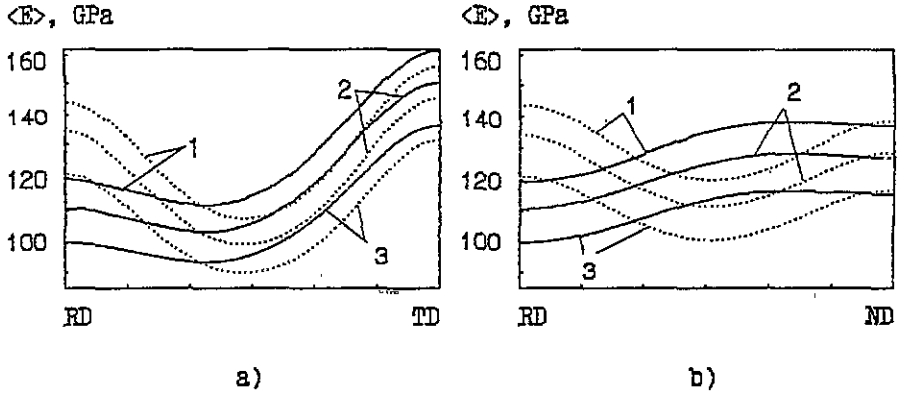


*Figure 4. Angular dependences of Young's modulus for a direction in (a) the* RD–TD *and (b)* the RD–ND planes for 79 K (curves 1), 300 K (curves 2) and 500 K (curves 3): ——, anisotropy for copper plates rolled at 77 K; ·····, anisotropy for copper plates rolled at 300 K.

The model three-dimensional ODFs are presented in figure 2 as two-dimensional sections with the $\varphi_2$ = constant planes. The even parts of the series expansion of the model ODFs were determined to correspond well to the ODFs reconstructed from the experimental pole

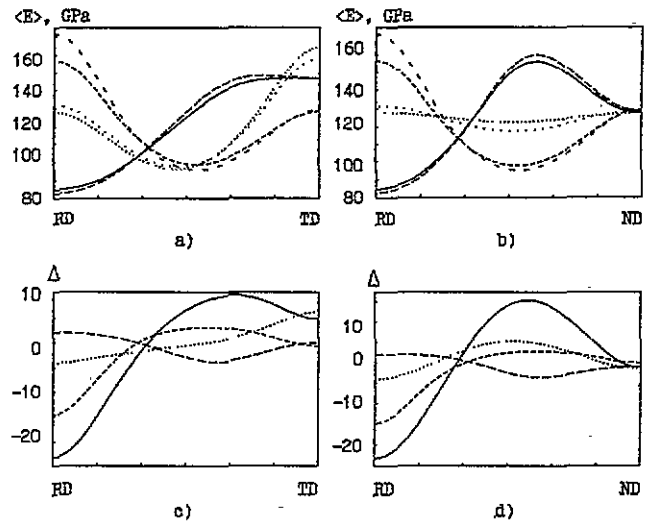


**Figure 5.** Angular dependences of Young's modulus for a direction in the (a) RD–TD and (b) RD–ND planes for different texture components: ·····, $\{110\}\langle 1\bar{1}2\rangle|1\bar{1}1|$ in copper rolled at 77 K; · · · ·, $\{110\}\langle 1\bar{1}2\rangle|1\bar{1}1|$ in copper rolled at 300 K; ----, $\{112\}\langle 11\bar{1}\rangle|111|$ in copper rolled at 77 K; – – –, $\{112\}\langle 11\bar{1}\rangle|111|$ in copper rolled at 300 K; ——, $\{110\}\langle 001\rangle|110|$ in copper rolled at 77 K; — — —, $\{110\}\langle 001\rangle|110|$ in copper rolled at 300 K. (c), (d) The angular dependences of Δ (GPa) in the same planes for the following components: ·····, $\{110\}\langle 1\bar{1}2\rangle|1\bar{1}1|$; ----, $\{112\}\langle 11\bar{1}\rangle|111|$; – – –, $\{110\}\langle 001\rangle|110|$; ——, the total texture.

figures by the Bunge–Roe technique [9]. Note that we analyse peculiarities of different texture component contributions to the property anisotropy; for details of experimental verification of the model the reader should consult [8, 9].

The averaged $\langle S_{ijkl}\rangle$-values are presented in table 2 with the use of the routine notation of a four-rank tensor by a two-dimensional $6 \times 6$ matrix. The single-crystal values $S^0_{ijkl}$ were taken from [14] for 79 and 300 K and were calculated on the basis of the results of [15] for 500 K.

In figure 3 the three-dimensional images of Young's modulus are presented for different types of the texture under consideration and for different components. The spacing of any surface point with respect to the reference point is proportional to Young's modulus $\langle E\rangle$ in this direction. As is obvious the anisotropy in the separate components is more pronounced than that for the total texture.

Note that we consider two types of temperature effect on the anisotropy, namely the effect of the rolling temperature (77 and 300 K) and the effect of the measurement temperature (79, 300 and 500 K). Only textural changes are taken into account.

The measurement temperature effect on the anisotropy of Young's modulus for the RD–TD and RD–ND planes is shown in figure 4. Here TD is the transverse direction, and ND is the normal direction. The deformation temperature is clearly seen to affect substantially the anisotropy of Young's modulus mainly in the RD and slightly in the TD and ND. This is caused by the decrease in volume fraction of the $\{112\}\langle 11\bar{1}\rangle|111|$ component (see table 1) in the deformation texture of copper rolled at $T_d = 77$ K, i.e. of the component having the maximum value of Young's modulus in the RD. The angular dependence of Young's modulus in the RD–TD plane of the $\{110\}\langle 1\bar{1}2\rangle|1\bar{1}1|$ component is almost symmetric to that for the $\{112\}\langle 11\bar{1}\rangle|111|$ component with respect to a direction making an angle of 45°

with the RD, (figure 5(a)). The effect of the spread magnitude of separate components on the anisotropy is easily seen from figures 5(c) and 5(d) where the angular dependences $\Delta = \langle E \rangle^{c} - \langle E \rangle^{b}$ are shown for three main texture components and for the total value of Young's modulus. The superscript c indicates a component in the texture of copper rolled at 300 K and the superscript b indicates the same component in the texture of copper rolled at 77 K. In other words this is the dependence of the deformation temperature effect on the measurement temperature. From figure 5 it is seen that the magnitude of spread of the $\{112\}\langle 11\bar{1}\rangle|111|$ component has no effect on Young's modulus in the TD and this holds also for the $\{110\}\langle 1\bar{1}2\rangle|1\bar{1}1|$ component in a direction making an angle of about 55° with the RD in the RD–TD plane. This correlates with locations of the exit of the {110} poles for the components under consideration.

Values of the elastic properties in directions out of the sheet plane must be known in order to calculate the stress and strain state of the anisotropic plates [16]. However, the experimental measurement of these values under sufficiently low thicknesses of the plates presents great difficulties. In this case, one may use the theoretical calculations, e.g. in the framework of the approach presented here.

The analysis of contributions of separate components to the total anisotropy shows that Young's modulus can be varied by the texture in the RD and to a smaller extent in the TD and the ND in the case of rolled copper.

In this paper the results of calculations in the Reuss approximation are presented, since only relative changes in the elastic properties and the contributions of separate texture components were of basic interest to us, but their precise magnitudes were not.

## Acknowledgments

This study was supported by the Ukrainian State Science and Technology Committee under project 4/339.

## References

[1] Dnieprenko V N, Larikov L N and Shchiritca A I 1988 *Problemy prochnosti* 2 61
[2] Dnieprenko V N, Larikov L N and Shchiritca A I 1986 *Metallofizika* 8 87
[3] Bunge H J 1968 *Krist. Tech.* 3 431
[4] Bunge H J (ed) 1987 *Theoretical Methods of Texture Analysis* (Oberursel: DGM Informationsgesellschaft)
[5] Wassermann G and Grewen J 1962 *Texturen-Metallischer Werkstoffe* (Berlin: Springer)
[6] Dnieprenko V N, Larikov L N and Stoyanova E N 1982 *Metallofizika* 4 58
[7] Dnieprenko V N 1993 *Proc. 10th Int. Conf. on Textures of Materials (Clausthal, 1993)* (Clausthal: Technische Universität) p 88
[8] Divinski S V and Dnieprenko V N 1993 *Textures Microstruct.* 22 73
[9] Dnieprenko V N and Divinski S V 1992 *Scr. Metall.* 27 1617
[10] Bunge H J 1969 *Mathematische Methoden der Texturanalyse* (Berlin: Akademie)
[11] Mathies S 1981 *Cryst. Res. Technol.* 16 1061
[12] Nikolaev D I and Savyolova T I 1992 *Textures Microstruct.* 19 9
[13] Hu H and Goodman S R 1963 *Trans. Metall. Soc. of AIME* 227 627
[14] Overton W G and Caffeny J 1955 *Phys. Rev.* 98 969
[15] Soma T, Hosaka T and Kagaya H-M 1987 *Phys. Status Solidi* b 141 K21
[16] McClintock F A and Argon A S 1966 *Mechanical Behavior of Materials* (Don Mills, Ontario: Addison-Wesley (Canada))